CROATICA CHEMICA ACTA
CCACAA **78** (2) 151–158 (2005)

ISSN-0011-1643
CCA-2991
Original Scientific Paper

Annotation of Transmembrane Segments of Experimentally Solved Bacterial Porins and Adhesins*

Damir Zucić

School of Medicine, University of Osijek, J. Huttlera 4, HR-31000 Osijek, Croatia
(E-mail: zucic@garlic.mefos.hr)

RECEIVED MAY 18, 2004; REVISED OCTOBER 29, 2004; ACCEPTED NOVEMBER 2, 2004

Keywords
porins
transmembrane segments
porin insertion model

The transmembrane parts of 16 porins of known structure were precisely annotated using Garlic, the membrane protein visualization program. Transmembrane preferences were obtained for 20 standard amino acids. The statistical data were combined with experimental knowledge about porin insertion to prepare the model of porin insertion into the outer membrane.

INTRODUCTION

The outer membrane of Gram-negative bacteria is rich in porins and adhesins, the β barrel-forming integral membrane proteins. Barrel-forming proteins are interesting as channels for drug delivery into bacterial cells, as possible targets for blocking of uptake channels which may lead to bacterial cell starvation and as templates for design of artificial membrane channels. Artificial β-barrel proteins may even find applications in material science, for example, to control the enzyme reaction kinetics.

Porins are inserted from the periplasmic space to the outer membrane, with polar loops on the extracellular side of the final structure. Up to now, the theoretical model of porin insertion into membrane was not available. It was experimentally shown that spontaneous, thermodynamically driven insertion of a small porin is possible, without any protein insertion machinery.[1]

Currently, 16 different structures of bacterial porins and adhesins have been experimentally solved and sequence databases, like PIR,[2] already contain more than thousand sequences which are annotated as belonging to bacterial outer membranes. A waste amount of data coming from genomic projects will significantly increase the number of putative porins.

A number of secondary structure prediction servers[3–7] may be found on the Internet with capability to predict the secondary structure and topology of the helix-bundle membrane proteins. However, most of these servers are unable to recognize the β-barrel membrane proteins and to distinguish them from soluble proteins, due to very similar average hydrophobicities of porins and soluble proteins.

Most of the existing protein secondary structure prediction methods require a database of precisely annotated sequences of experimentally solved porins. Transmembrane sequence fragments of porins are short, thus wrong annotations of transmembrane portions of porins may complicate both the prediction and the comparison of different prediction methods. Just nine residues in extented conformation are enough to traverse the entire membrane thickness. The lack of precise annotations is one of the main reasons why the prediction methods for porins are

* Dedicated to Dr. Edward C. Kirby on the occasion of his 70th birthday.

much less developed than prediction methods for helix bundle membrane proteins.

While transmembrane domains of helix-bundle proteins contain at least 14 residues[8] and typically about 20 residues, most of which are hydrophobic residues, the hydrophobic core of the outer membrane of Gram-negative bacteria is sometimes spanned by just 7 residues. Further, every second side chain in a strand which takes part in a formation of the barrel wall is oriented toward the barrel interior and thus not necessarily exposed to a hydrophobic environment. For this reason, the average hydrophobicity of transmembrane segments is not very large and in some cases five consecutive polar residues may be found in a transmembrane part of the barrel. For example, the polar sequence motif SSRSR may be found in the second strand of porin from Rhodobacter capsulatus.

In the previous work,[9] a method for determination of transmembrane portions of membrane proteins was described. In this work, this method was applied to 16 non-homologous, experimentally solved beta-barrel structures. The annotated transmembrane regions were analyzed to obtain the distribution of residues and residue preferences across the hydrophobic portion of the outer membrane. The characteristic residue patterns were combined with the experimental knowledge about insertion of porins to prepare the theoretical model for insertion of porin into the outer membrane.

METHODS

The Protein Data Bank[10] (PDB) contains more than 40 structures of porins and barrel-forming adhesins. However, many of these proteins are closely related, so the total number of structures with low pairwise sequence identity is just 16. Table I contains the list of useful porins and adhesins.[11–26]

All selected proteins are inserted from the periplasmic space to the outer membrane. In other reviews,[27,28] the alpha-hemolysin toxin was included in the list. In this work, the alpha hemolysin was discarded for three reasons:

(i) This toxin is inserted into the membrane from the extracellular side;

(ii) The composition of the membrane into which the alpha-hemolysin inserts is different from the composition of the outer membrane of Gram-negative bacteria;

(iii) While for the selected proteins a single polypeptide chain forms the β-barrel, the alpha hemolysin is a multimeric proteins, consisting of seven equal chains.

At present, there is no detailed theoretical model for porin insertion into the membrane. The precise information about the transmembrane, extracellular and periplasmic portions for a number of porins was used to build the theoretical model of porin insertion. Some of the previous works[18,27–29] with annotations of porin structures were based on subjective estimate of the transmembrane portion of porins.

TABLE I. Selected porins of known structure

PROTEIN	SOURCE	PDB CODE	STRANDS
Porin	*Rhodobacter capsulatus*	2POR	16
OmpF	*Escherichia coli*	1OPF	16
Porin	*Rhodopseudomonas blastica*	1PRN	16
OmpK36	*Klebsiella pneumoniae*	1OSM	16
Omp32	*Comamomonas acidovorans*	1E54	16
Maltoporin	*Escherichia coli*	1MAL	18
ScrY	*Salmonella typhimurium*	1A0S	18
OmpA	*Escherichia coli*	1BXW	8
OmpX	*Escherichia coli*	1QJ8	8
FhuA	*Escherichia coli*	2FCP	22
FepA	*Escherichia coli*	1FEP	22
FecA	*Escherichia coli*	1KMO	22
OMPLA	*Escherichia coli*	1QD5	12
OmpT	*Escherichia coli*	1I78	10
OpcA	*Neisseria meningitidis*	1K24	10
apoBtuB	*Escherichia coli*	1NQE	22

In this work, a previously described method,[9] implemented in a molecular visualization program Garlic, was applied on a set of 16 selected porins, available from the Protein Data Bank. This data set was inspected twice. In the first passage, the thickness of the hydrophobic part of the outer membrane was estimated, based on a distance between two rings of aromatic residues, which are common among porins. The value of 2 nm was found to be suitable for the second passage.

In the second passage, the built-in command MEMBRANE was used to attach the membrane model to each porin. The transmembrane parts of strands were carefully inspected. For each porin, a separate spreadsheet was prepared, listing the transmembrane portions, the periplasmic loops and from three to seven residues on the extracellular side from each strand.

As some extracellular loops and loops which are residing in barrel interior are quite long, only parts of these long strands and loops were included (up to seven residues), to preserve the clarity and to reduce the size of the schemes. The complete extracellular loops may be easily obtained from the protein sequences, because each scheme contains both the residue name and serial number.

The most important difficulty in the assignment of porin secondary structure comes from the fact that in almost every porin, one side of the barrel consists of longer strands which are usually highly ordered, while the other side consists of shorter strands which are often distorted by β-bulges. Further, the strands which make distorted part of the barrel wall are also displaying a larger tilt angle. As a consequence, the number of residues required to traverse the hydrophobic part of the outer membrane is larger for distorted (shorter) side of the barrel. While only seven residues are typically required to traverse the hydrophobic part of the membrane

on the ordered side of the barrel, on the other side eleven residues are typically required.

As the output data were written to a rectangular scheme (spreadsheet), with strands placed in vertical columns, it was impossible to simultaneously align the aromatic residues in the upper ring (extracellular side) and the aromatic residues in the bottom ring of aromatic residues. For convenience, only the top ring was properly aligned.

RESULTS AND DISCUSSION

Figure 1 shows the secondary structure and topology assignment for OmpA adhesin from Escherichia. This example was chosen just because this protein is relatively small; the assignments for all 16 proteins are too extensive to be presented here. The complete data set may be found on the web page: http://garlic.mefos.hr/porins in two formats: .html and .xls (for downloading). Both versions are suitable for printing. Each barrel is »unwound« and shown as a separate scheme. Transmembrane strands are listed from right to left, with the periplasmic loops at the bottom of each scheme and extracellular loops at the top. Most of the extracellular loops are truncated to retain the simplicity of the scheme. Cork regions and loops which reside in the barrel interior are not shown.

1BXW		8 STRANDS		OMPA, *E. COLI*				
8	7	6	5	4	3	2	1	
⋮	⋮	⋮	⋮	⋮	⋮	⋮	⋮	
ILE 153	ALA 150	GLY 112	SER 108	GLY 70	LYS 64	GLY 28	GLY 22	P6
GLY 154	ASP 149	LYS 113	TYR 107	ALA 71	TYR 63	PRO 29	THR 21	P5
THR 155	GLY 148	ASN 114	THR 106	TYR 72	PRO 62	THR 30	ASP 20	P4
ARG 156	ILE 147	HIS 115	ASP 105	LYS 73	MET 61	HIS 31	HIS 19	P3
PRO 157	ASN 146	ASP 116	ALA 104	ALA 74	ARG 60	GLU 32	TYR 18	P2
ASP 158	ASN 145	THR 117	ARG 103	GLN 75	GLY 59	ASN 33	GLN 17	P1
ASN 159	THR 144	GLY 118	TRP 102	GLY 76	LEU 58	LYS 34	SER 16	P0
GLY 160	TRP 143	VAL 119	VAL 101	VAL 77	TRP 57	LEU 35	TRP 15	P-1
MET 161	GLN 142	SER 120	MET 100	GLN 78	ASP 56	GLY 36	GLY 14	P-2
LEU 162	TYR 141	PRO 121	GLY 99	LEU 79	TYR 55	ALA 37	LEU 13	P-3
SER 163	GLU 140	VAL 122	GLY 98	THR 80	GLY 54	GLY 38	LYS 12	P-4
LEU 164	LEU 139	PHE 123	LEU 97	ALA 81	MET 53	ALA 39	ALA 11	P-5
GLY 165	ARG 138	ALA 124	ARG 96	LYS 82	GLU 52	PHE 40	GLY 10	P-6
VAL 166	THR 137	GLY 125	THR 95	LEU 83	PHE 51	GLY 41	THR 9	P-7
SER 167	ALA 136	GLY 126	TYR 94	GLY 84	GLY 50	GLY 42	TYR 8	
TYR 168	ILE 135	VAL 127	ILE 93	TYR 85	VAL 49	TYR 43	TRP 7	
ARG 169	GLU 134	GLU 128	ASP 92	PRO 86	TYR 48	GLN 44	THR 6	
PHE 170	PRO 133	TYR 129	LEU 91	ILE 87	PRO 47	VAL 45	ASN 5	
GLY 171	THR 132	ALA 130	ASP 90	THR 88		ASN 46	ASP 4	
		ILE 131	ASP 89					

Figure 1. The secondary structure and topology assignment for OmpA from *Escherichia coli*. Residue numbers match the numbers in the corresponding PDB entry (1BXW). Thick red line outlines the transmembrane strands. The hydrophobic membrane core is below the thick blue line, while the extracellular polar part of the membrane is above this line. Residue positions relative to the border between the hydrophobic core and polar region of the membrane are given in green rectangles.

The sequence numbers match the serial numbers in the corresponding PDB entries. There are no deletions and insertions: some serial numbers are missing and some other serial numbers are used more than once because some of the original PDB files have homologous numbering.

The inner leaflet of the outer membrane of Gram negative bacteria is made mostly of phospholipid molecules, while the outer leaflet is made mostly of lipopolysaccharides (LPS), The thick, horizontal blue line shows the border between the hydrophobic core (hydrophobic tails of fatty acids) and the polar part of the outer leaflet (polar heads of fatty acids and polysaccharide chains). It is assumed that this border is close to the upper ring of aromatic residues. Two such rings are characteristic for porins: one on the extracellular (upper) side and another one on the periplasmic (bottom) side.

The broken red line is drawn to distinguish side chains which are outside the barrel from side chains which are inside the barrel. The vertical red line to the right of the residue name marks the side chain which points outwards.

A column of green rectangles is used to define the positions of residues with respect to the border between the hydrophobic core and the polar part of the outer leaflet. The waste majority of side chains at the position P_0 is pointing inwards. The most frequent residues at the position P_{-1} are aromatic residues. Note that positions of sides chains with respect to hydrophobic/polar region border are always listed in direction from the periplasmic side towards the extracellular side, though every second strands is pointing in the opposite direction.

Figure 2 shows the statistical overview for all 16 proteins, with a total of 252 strands. A total number of side chains of each type was counted for 14 positions, from P_{-7} to P_6. The seleno-methionine, which was artificially introducted into some structures, was counted as ordinary methionine. No other exotic residues were found. The residues are sorted alphabetically (from top to bottom). Some loops were too short to fill all 14 positions, so there are some missing residues. The most frequent residues at a given position are marked by yellow rectangles and other frequent residues are marked by green rectangles. The most frequent residue in the transmembrane region if glycine.

The transmembrane strands are tilted with respect to the barrel axis. A different tilt angle results in different

	P-7	P-6	P-5	P-4	P-3	P-2	P-1	P0	P1	P2	P3	P4	P5	P6	TOTAL
ALA	25	20	40	21	25	23	21	19	3	23	14	19	25	11	289
ARG	1	29	0	23	0	4	0	9	28	14	21	16	13	13	171
ASN	12	22	2	10	4	13	0	18	30	29	21	21	16	19	217
ASP	5	14	2	5	0	23	0	18	41	19	30	25	18	24	224
CYS	0	0	0	0	0	0	0	0	1	0	0	0	0	0	1
GLN	5	12	2	13	2	18	0	24	27	11	10	11	8	11	154
GLU	1	20	1	12	0	17	0	16	20	13	12	14	10	14	150
GLY	18	33	25	54	24	37	11	41	15	27	15	29	24	24	377
HIS	7	2	0	2	2	1	9	2	4	5	5	0	3	0	42
ILE	18	3	13	4	19	6	13	6	1	12	7	7	12	7	128
LEU	27	4	56	10	52	12	24	15	1	7	7	8	10	8	241
LYS	3	21	2	11	0	6	0	5	30	12	34	12	19	11	166
MET	6	3	8	3	6	10	6	8	1	3	2	2	2	2	62
PHE	20	7	18	2	25	6	28	3	3	4	6	7	7	7	143
PRO	6	1	6	0	6	0	5	1	0	4	6	4	10	10	59
SER	6	19	11	31	4	30	0	12	25	24	31	20	17	15	245
THR	14	23	12	23	15	21	5	25	21	21	7	23	17	17	244
TRP	9	1	5	4	4	4	30	3	1	3	1	5	6	3	79
TYR	34	6	10	17	26	17	67	14	0	10	14	10	6	15	246
VAL	32	11	39	7	38	4	33	13	0	11	6	12	9	8	223
Total	249	251	252	252	252	252	252	252	252	252	249	245	232	219	3461

Figure 2. The number of residues of a given type at 14 positions (from P_{-7} to P_6). Position P_0 defines the border between the hydrophobic core of the outer membrane and the polar part of the outer leaflet. Position P_{-7} is close to the periplasmic space, while P_6 is close to the extracellular space. Some strands were too short so there are missing residues at positions close to the edge.

number of residues required to traverse the hydrophobic core of the outer membrane. The most frequent residue facing the membrane in the central region of the hydrophobic core (P_{-3} and P_{-5}) is leucine; valine is also very frequent. Closer to the edge of the hydrophobic core (P_{-1} and P_{-7}), tyrosine is the most frequent residue exposed to the membrane and other aromatic residues are also frequent. Charged and zwitterion residues are very common at positions P_1 and P_3, which are exposed to the polar part of the outer leaflet of the outer membrane.

Glycine is the most frequent or the second most frequent residue at positions in the barrel interior, over the entire length of barrel wall (P_{-6}, P_{-4}, P_{-2}, P_0, P_2, P_4, P_6). Most leucine and phenylalanine residues are located in the hydrophobic part of the membrane and few of these residues are found on the extracellular side. On the other hand, alanine is found frequently on both sides of the barrel wall, evenly distributed over the entire length of the barrel. The only exception is position P_1, which is reserved for polar residues. Hydrophobic residues (except glycine) are very rarely found at position P_1.

The following sequence motifs should be the most preferred transmembrane patterns in the region which is covers the positions from P_{-5} to P_{-1}:

[YWF]-x-[LV],

[LV]-x-[YWF],

[YWF]-x-[LV]-x-[LVAG] and

[LVAG]-x-[LV]-x-[YWF].

The patterns are written using PROSITE notation[30] and standard one letter codes. These patterns may be found in all 16 selected porins of known 3D structure. In the waste majority of cases, such patterns are found in transmembrane strands, but it is interesting to note that the same patterns may be found in cork regions and in long extracellular loops. These loops are long enough to cross the membrane as complete hairpins, each consisting of two strands and one turn on the periplasmic side. This lead to the hypothesis, that some of the extracellular loops and corks were part of the barrel in some early stage of porin insertion. The subsequent rearrangement of the inserted structure brought them to their final position, outside of the barrel wall, reducing the barrel size.

A distribution of membrane-exposed side chains in the transmembrane region shares some similarity with a simple hydrophobic hexapeptide, acetyl-Trp-Leu_5, which was shown to insert spontaneously into lipid bilayer membranes, forming β-sheet aggregates.[31]

In every porin, there are at least two strands which have four hydrophobic side chains exposed to the hydrophobic core followed of preceded by two polar side chains exposed to the polar part of the outer leaflet. In this work, threonine is counted as hydrophobic when exposed to the hydrophobic core. However, the same motif may be found in corks or long extracellular loops, even in the smallest proteins from the set of 16 proteins. This explains the failure of simple secondary structure prediction methods with porins, which consistently gave serious over-predictions.[32]

In a final conformation, every second side chain is placed inside the barrel interior. Depending on the local environment, these side chains may be exposed to the polar environment or protected from polar molecules. It is interesting to note, that positive side chains are rarely found at position P_{-2}, preferring positions P_{-4} and P_{-6}. On the other hand, negative side chains which are inside the barrel are most frequently found at position P_{-2}. Two positive side chains, separated by a single residue, may be found in each porin. This motif takes part in LPS binding.[33]

If looking from the extracellular side, the hydrophobic core is traversed by a number of hairpins. Each hairpin is made of two strands and a single turn. The length of a single hairpin may be calculated starting with the

TABLE II. Hairpin lengths

Hairpin length [residues]	Number of hairpins
12	2
13	0
14	1
15	1
16	3
17	0
18	12
19	13
20	6
21	15
22	6
23	15
24	5
25	13
26	1
27	7
28	3
29	6
30	0
31	1
TOTAL:	110

residue at position P_{-1} from the first strand and ending with the residue at the same position from the second strand. As the first and the last strand from each structure are not involved in hairpins which have turns on periplasmic side, the total number of hairpins from 16 structures is 110.

The shortest hairpin found in data set consists of 12 residues, while the longest consists of 31 residue. The number of hairpins of a given length, for each possible length between 12 and 31, is given in Table II. Most of the hairpins have the length between 18 and 25 residues.

It is interesting to investigate the average hydrophobicity of a porin, using a simple rectangular sliding window of 18 residues. This window width is suitable for most of the hairpins with turns on periplasmic side. The experimental hydrophobicity scale, based on whole-residue free energies of transfer from water to bilayer interface, was chosen to calculate the average hydrophobicity values.[34]

Figure 3 shows the average hydrophobicity for porin from *Rhodobacter capsulatus.* Small arrows are used to mark the positions of periplasmic turns in 3D structures. There is strong experimental evidence that porins have little ordered structure before insertion, thanks to the formation of the complex with chaperones and lipopolysaccharide molecules[35]. The sections of the unfolded chain which favor spontaneous insertion into the bilayer interface are visible as prominent peaks in Figure 3. There is no need to make any assumptions about sided hydrophobicity to predict the position of most periplasmic turns, using extremely simple model. This is valid for most porins, except the largest (consisting of 22 strands).

Porin Insertion Model

It was proven that porins pass through the periplasm before insertion to the outer membrane.[36] Experiments with OmpA showed that insertion of this porin is a multi-step proces, characterized by three partially inserted, membrane-bound intermediates.[37] The sequential insertion (hairpin by hairpin) is not possible as a spontaneous process, because this mechanism would require the translocation of hydrogen bond donors and acceptors from polar to hydrophobic environment.

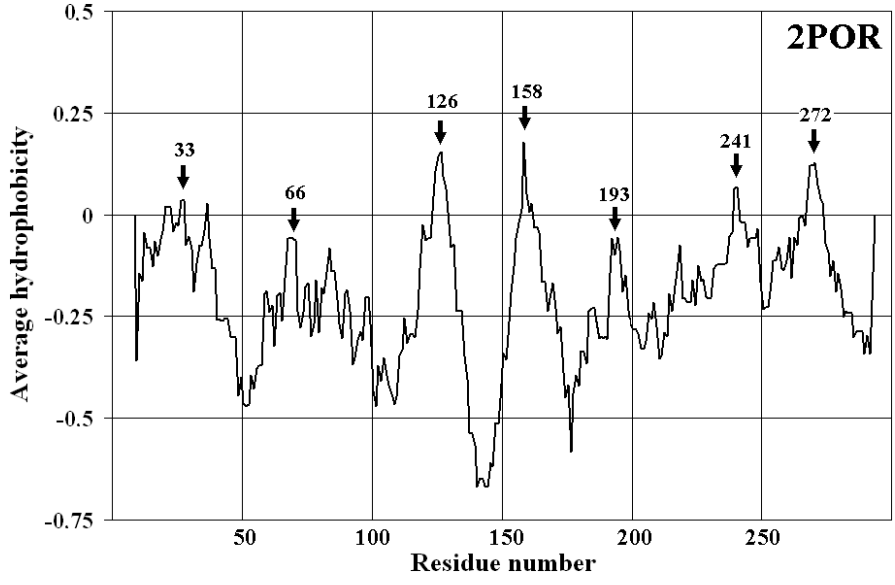

Figure 3. Average hydrophobicity for porin from *Rhodobacter capsulatus*. Black arrows are marking positions of periplasmic turns in 3D structure. Residue numbers of turn centers are written above arrows. The sliding window width was 18 residues.

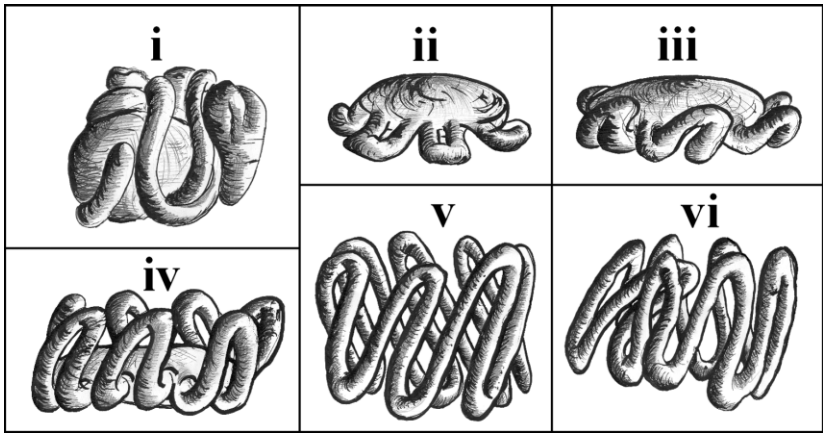

Figure 4. Theoretical model of porin insertion.

Time-resolved distance determination by fluorescence quenching showed that the barrel forms as it is inserted.[1] The β-sheet content increases as porin inserts deeper into the membrane. In the final structure, the sequence stretches rich in polar residues will be placed on the extracellular side. For example, a motif [RK]-x-[RK] is very polar, so it is should be permanently screened from the hydrophobic environment during the translocation through the hydrophobic core. The following theoretical model was designed to explain the insertion of porin into the outer membrane (Figure 4):

(i) Porin approaches the outer membrane complexed with other protein molecules (like Skp chaperone) and LPS, in almost unfolded form. This assumption is based on experimental evidence;[35]

(ii) The most hydrophobic loops are leading the insertion of porin into polar bilayer interface. A ring of short, hydrophobic loops forms around a molten disc. Some of these loops (Figure 3) will play the role of periplasmic loops in the final structure. For a typical porin, it is easy to recognize these loops by drawing a simple average hydrophobicity plot, using a sliding window of seven residues. A shallow penetration of the most hydrophobic loops corresponds to the second step of the multistep insertion process experimentally discovered by Kleinschmidt *et al.*;[37]

(iii) A shallow but wide barrel begins to form around the molten disc, by establishment of hydrogen bonds between the hydrophobic loops, thus being suitable to penetrate into the hydrophobic core. It was experimentally shown that barrel formation is synchronized with insertion;[38]

(iv) The barrel becomes deeper, penetrating further into the hydrophobic core. During the insertion process, the interstrand hydrogen bonds are created in the growing barrel wall. Free hydrogen bond donors and acceptors interact with solvent and neighboring side chains inside the barrel cavity, being protected from the hydrophobic core;

(v) The most polar loops migrate through the barrel interior to the polar region of the outer leaflet. During the entire insertion process, these loops are not exposed to the hydrophobic core. This explains one of the most peculiar facts about porins: porins may be spontaneously inserted from the periplasmic side, yet the most polar parts of porins are on the extracellular side of the final structure. The migration of polar loops through the barrel interior is consistent with the experimental facts that insertion is a spontaneous, thermodynamically driven process,[1] because these loops are permanently screened from the hydrophobic core. The external migration will require some other screening mechanism, like another protein;

(vi) Part of the barrel wall collapses, due to the surface tension forces and thermal agitation. The net surface tension forces may transiently become strong because the barrel is open for a short period of time, allowing the leakage of solvent. The strands which remain inside the barrel wall form new hydrogen bonds, while the collapsed loops interact with solvent molecules and polar side chains in the barrel interior. The barrel becomes narrower but the central opening is closed by one or more loops. The breaking of hydrogen bonds which held collapsing loops in the barrel wall is initiated on the periplasmic side. The ends of collapsed loops are close to the extracellular end of the barrel wall. It is important to note that most of the loops in the barrel interior of experimentally solved porins are long enough to fit into the barrel in a form of two strands connected with a periplasmic turn. The same is valid for many external occlusion loops.

The exposed model is consistent with the most intriguing facts about porins: spontaneous insertion with no insertion machinery, presence of charged side chains and very polar sequence stretches on the extracellular side of the final structure and formation of secondary structure during insertion.

It should be noted that glycine is very abundant on the inner side of the barrel wal. It is generaly thought to be a consequence of steric constraints, but in the model exposed above glycine and other small residues are fa-

vored because of flexibility, which allows sharp bending of loops during barrel formation. It also explains why beta-branched residues are rare in barrel interior, though they are smaller than tyrosine, which plays important role in the barrel interior of some porins. The model explains the failure of simple secondary structure prediction methods with porins: the over-predictions and under-predictions may be, in fact, correct predictions of a transient state of the porin. The barrel rearrangement causes some hairpins to be excluded from barrel walls and some other hairpins to become partially rearranged. The oligomerization may also induce some rearrangement of the barrel.

Acknowledgment. – This work was supported by the Croatian Ministry of Science and Technology Grant 0219031.

REFERENCES

1. L. K. Tamm, A. Arora, and J. Kleinschmidt, *J. Biol. Chem.* **276** (2001) 32399–32402.
2. C. H. Wu, H. Huang, L. Arminski, J. Castro-Alvear, Y. Chen, Z.-Z. Hu, R. S. Ledley, K. C. Lewis, H.-W. Mewes, B. C. Orcutt, B. E. Suzek, A. Tsugita, C. R. Vinayaka, L.-S. L. Yeh, J. Zhang, and W. C. Barker, *Nucleic Acids Res.* **30** (2002) 35–37.
3. A. Krogh, B. Larsson, G. von Heijne, and E. L. L. Sonnhammer, *J. Mol. Biol.* **305** (2001) 567–580.
4. T. Hirokawa, S. Boon-Chieng, and S. Mitaku, *Bioinformatics* **14** (1998) 378–379.
5. B. Rost, R. Casadio, P. Fariselli, and C. Sander, *Protein Sci.* **4** (1995) 521–533.
6. D. Juretić, D. Zucić, B. Lučić, and N. Trinajstić, *Computers Chem.* **22** (1998) 279–294.
7. D. Juretić, A. Jerončić, and D. Zucić, *Croat. Chem. Acta* **72** (1999) 975–997.
8. M. Monné, I. Nilsson, A. Elofsson, and G. von Heijne, *J. Mol. Biol.* **293** (1999) 807–814.
9. D. Zucić and D. Juretić, *Croat. Chem. Acta* **77** (2004) 403–414.
10. H. M. Berman, T. Battistuz, T. N. Bhat, W. F. Bluhm, P. E. Bourne, K. Burkhardt, Z. Feng, G. L. Gilliland, L. Iype, S. Jain, P. Fagan, J. Marvin, D. Padilla, V. Ravichandran, B. Schneider, N. Thanki, H. Weissig, J. D. Westbrook, and C. Zardecki, *Acta Cryst.* **D58** (2002) 899–907.
11. M. S. Weiss, U. Abele, J. Weckesser, W. Welte, E. Schiltz, and G. E. Schulz, *Science* **254** (1991) 1627–1630.
12. S. W. Cowan, T. Schirmer, G. Rummel, M. Steiert, R. Ghosh, R. A. Pauptit, J. N. Jansonius, and J. P. Rosenbusch, *Nature* **358** (1992) 727–733.
13. A. Kreusch, A. Neubueser, E. Schiltz, J. Weckesser, and G. E. Schulz, *Protein Sci.* **3** (1994) 58–63.
14. R. Dutzler, G. Rummel, S. Alberti, S. Hernandez-Alles, P. Phale, J. Rosenbusch, V. Benedi, and T. Schirmer, *Structure (London)* **7** (1999) 425–434.
15. K. Zeth, K. Diederichs, W. Welte, and H. Engelhardt, *Structure Fold. Des.* **8** (2000) 981–992.
16. T. Schirmer, T. A. Keller, Y.-F. Wang, and J. P. Rosenbusch, *Science* **267** (1995) 512–514.
17. D. Forst, W. Welte, T. Wacker, and K. Diederichs, *Nat. Struct. Biol.* **5** (1998) 37–46.
18. A. Pautsch and G. E. Schulz, *Nat. Struct. Biol.* **5** (1998) 1013–1017.
19. J. Vogt and G. E. Schulz, *Structure (London)* **7** (1999) 1301–1309.
20. A. D. Ferguson, E. Hofmann, J. W. Coulton, K. Diederichs, and W. Welte, *Science* **282** (1998) 2215–2220.
21. S. K. Buchanan, B. S. Smith, L. Venkatramani, D. Xia, L. Esser, M. Palnitkar, R. Chakraborty, D. van der Helm, and J. Deisenhofer, *Nat. Struct. Biol.* **6** (1999) 56–63.
22. A. D. Ferguson, R. Chakraborty, B. S. Smith, L. Esser, D. van der Helm, and J. Deisenhofer, *Science* **295** (2002) 1715–1719.
23. H. J. Snijder, I. Ubarretxena-Belandia, M. Blaauw, K. H. Kalk, H. M. Verheij, M. R. Egmond, N. Dekker, and B. W. Dijkstra, *Nature* **401** (1999) 717–721.
24. L. Vandeputte-Rutten, R. A. Kramer, J. Kroon, N. Dekker, M. R. Egmond, and P. Gros, *Embo J.* **20** (2001) 5033–5039.
25. S. M. Prince, M. Achtman, and J. P. Derrick, *Proc. Nat. Acad. Sci. USA* **99** (2002) 3417–3421.
26. D. P. Chimento, A. K. Mohanty, R. J. Kadner, and M. C. Wiener, *Nat. Struct. Biol.* **10** (2003) 394–401.
27. W. C. Wimley, *Protein Sci.* **11** (2002) 301–312.
28. W. C. Wimley, *Curr. Opin. Struct. Biol.* **13** (2003) 404–411.
29. R. Koebnik, K. P. Locher, and P. Van Gelder, *Mol. Microbiol.* **37** (2000) 239–253.
30. P. Bucher and A. Bairoch, *Proc. Int. Conf. Intell. Syst. Mol. Biol.* (1994) 53–61.
31. W. C. Wimley, K. Hristova, A. S. Ladokhin, L. Silvestro, P. H. Axelsen, and S. H. White, *J. Mol. Biol.* **277** (1998) 1091–1110.
32. G. von Heijne in: M. J. Sternberg (Ed.), *Protein Structure Prediction*, Oxford University Press, New York, 1996, pp. 101–109.
33. A. D. Ferguson, W. Welte, E. Hoffman, B. Lindner, O. Holst, J. W. Coulton, and K. Diederichs, *Structure Fold. Des.* **8** (2000) 585–592.
34. S. H. White and W. C. Wimley, *Biochim. Biophys. Acta* **1376** (1998) 339–352.
35. P. V. Bulieris, S. Behrens, O. Holst, and J. H. Kleinschmidt, *J. Biol. Chem.* **278** (2003) 9092–9099.
36. E. F. Eppens, N. Nouwen, and J. Tommassen, *The EMBO Journal* **16** (1997) 4295–4301.
37. J. Kleinschmidt and L. K. Tamm, *Biochemistry* **35** (1996) 12993–1300.
38. J. Kleinschmidt and L. K. Tamm, *J. Mol. Biol.* **324** (2002) 319–330.

SAŽETAK

Označavanje transmembranskih dijelova eksperimentalno riješenih struktura bakterijskih porina i adhezina

Damir Zucić

Transmembranski dijelovi 16 porina poznate strukture precizno su označeni pomoću programa Garlic, namijenjenog vizualizaciji membranskih proteina. Ispitane su transmembranske sklonosti 20 standardnih aminokiselina. Statistički podaci kombinirani su s eksperimentalnim podacima o ugradnji porina, radi izrade modela ugradnje porina u vanjsku membranu.